SUBSEQUENT ATMOSPHERIC CORRECTION OF THE CLARA-SAL SURFACE ALBEDO TIME SERIES 1982-2009

Terhikki Manninen, Aku Riihelä and Emmihenna Jääskeläinen

Finnish Meteorological Institute, P.O. Box 503, FI-00101 Helsinki, Finland

Abstract

The recently presented global surface albedo time series CLARA-SAL covering the years 1982-2009 was processed using a constant aerosol optical depth (τ_{550} = 0.1). In this study a postprocessing method based only on aerosol optical depth values and land cover information is presented for taking into account thicker atmosphere. Simulations of the postprocessing are carried out to quantify the accuracy. The postprocessed albedo accuracy is lowest for grassland and the error increases essentially linearly with the aerosol optical depth.

INTRODUCTION

The recently presented global surface albedo time series CLARA-SAL covering the years 1982-2009 is processed using constant atmospheric optical depth (τ_{550} = 0.1), because at the time of the processing of the SAL time series there was not sufficient aerosol optical depth (AOD) data available globally during all the years in question to support a high quality atmospheric correction. As the AOD value used for every image and pixel is the same, it is possible to carry out a postprocessing of the atmospheric correction, if one has AOD-information in the area of interest. The postprocessing is based on simulations of the effect on the erroneous AOD value on the surface albedo and the atmospheric correction procedure carried out in the SAL processing, i.e. the running the SMAC (Simplified Method for Atmospheric Correction) algorithm. It is shown, that albedo retrieval in areas of moderate AOD values does not markedly suffer from the constant AOD assumption. However, rainforests and other areas with thick atmosphere are certainly affected by carrying out the atmospheric correction using an AOD value far from the true one. Example cases are calculated 1) to demonstrate how to retroactively improve the atmospheric correction and 2) to quantify the loss in accuracy due to the constant atmosphere assumption.

ATMOSPHERIC CORRECTION

The atmospheric correction of the current CLARA-A1-SAL time series is based on the SMAC routine (Rahman and Dedieu 1994). For every pixel the constant value τ_{550} = 0.1 is used for the aerosol optical depth (AOD) at wavelength 550 nm. The values for water vapour content are calculated in the CLARA product chain and expected to be representative of the true values. The ozone concentration is taken to be constant: 0.35 atm-cm. Postprocessing of the surface albedo product is needed only, where the true value of τ_{550} is markedly larger than 0.1, like in Sahara or in rainforest areas. In the SMAC algorithm the relationship between the top of atmosphere (TOA) reflectance ρ_{TOA} and the surface reflectance ρ is

$$\rho_{TOA}(\theta_s,\theta_v,\Delta\varphi)=t_g(\theta_s,\theta_v,\Delta\varphi)\left\{\rho_a(\theta_s,\theta_v,\Delta\varphi)+\frac{T(\theta_s)T(\theta_v)\rho(\theta_s,\theta_v,\Delta\varphi)}{1-\rho(\theta_s,\theta_v,\Delta\varphi)S}\right\} \quad (1)$$

where t_g is the total gaseous transmission (both upward and downward paths), ρ_a is the atmospheric reflectance (a function of the optical properties of air molecules and aerosols as well as the

illumination/viewing geometry), $T(\theta s)$ is the atmospheric (scattering) transmission (downward), $T(\theta v)$ is the atmospheric (scattering) transmission (upward) and *S* is the spherical albedo of the atmosphere. The AOD value affects only the terms in the brackets. Details of the terms are described in the paper by Rahman and Dedieu (1994).

BROADBAND ALBEDO CALCULATION

The anisotropy correction of the CLARA-SAL algorithm (Riihelä et al, 2013) is based on the kernel model by Roujean et al. (1992) and Wu et al. (1995). The anisotropy of the reflectance ρ is then described by

$$\rho(\theta_s, \theta_v, \Delta\varphi) = k_0 + k_1 f_1(\theta_s, \theta_v, \Delta\varphi) + k_2 f_2(\theta_s, \theta_v, \Delta\varphi) \quad (2)$$

where subscript 0 denotes nadir reflectance, subscript 1 denotes geometrical scattering term, and subscript 2 denotes volume scattering term. The model is valid for the waveband over which its kernels are defined. The *k* terms are the geometric and volume scattering kernels, and the *f* terms are their associated viewing and illumination angle dependency functions. Likewise the anisotropy factor Ω is given by

$$\Omega(\theta_s, \theta_v, \Delta\varphi) = 1 + a_1 f_1(\theta_s, \theta_v, \Delta\varphi) + a_2 f_2(\theta_s, \theta_v, \Delta\varphi) \quad (3)$$

where $a_1 = k_1 / k_0$ and $a_2 = k_2 / k_0$. It should be noticed, that the values of the coefficients k_0, k_1 and k_2 depend on the wavelength as well as the land cover class. In the SAL algorithm the snow-free land classes are divided in four main types: barren, forest, crop and grass. The anisotropy factor is first used to normalize the surface reflectance to a common viewing and illumination geometry of zenith Sun, nadir view using (Li et al., 1996)

$$\rho(0,0,\Delta\varphi) = \frac{\Omega(0,0,\Delta\varphi)}{\Omega(\theta_s, \theta_v, \Delta\varphi)} \rho(\theta_s, \theta_v, \Delta\varphi) \quad (4)$$

By definition $\rho(0,0,\Delta\varphi)$ equals k_0. The spectral albedo $\alpha_i(\theta_s)$ is then

$$\alpha_i(\theta_s) = \rho_i(0,0,\Delta\varphi) + a_{i1} I_1(\theta_s) + a_{i2} I_2(\theta_s) \quad (5)$$

where *i* refers to either red or near infrared channel, I_1 and I_2 are integrals of f_1 and f_2 and the coefficients a_{i1} and a_{i2} are given in *Table 1*. Finally, the broadband albedo α (for other land cover classes than snow) is then obtained from the visible and near infrared band albedo values by (Liang, 2000)

$$\alpha = -0.3376 * \alpha_{\text{red}}^2 - 0.2707 * \alpha_{\text{nir}}^2 + 0.7074 * \alpha_{\text{red}} * \alpha_{\text{nir}} + 0.2915 * \alpha_{\text{red}} + 0.5256 * \alpha_{\text{nir}} + 0.0035 \quad (6)$$

We limit here the study in the snow-free land cover classes, because the thick atmosphere appears mostly in such areas. For snow covered areas the assumption τ_{550} = 0.1 is usually sufficiently close to the real value to provide broadband albedo estimates at reasonable accuracy.

Land cover	a_{red1}	a_{red2}	a_{nir1}	a_{nir2}
Barren	**0.21**	**1.629**	**0.212**	**1.512**
Cropland	**0**	**3.622*NDVI$^{0.539}$**	**0**	**1.62*NDVI$^{0.109}$**
Forest	**0**	**3.347*NDVI$^{0.153}$**	**0**	**1.830*NDVI$^{-0.105}$**
Grassland	**1.335*exp(-11.39*NDVI)**	**-0.493+14.94*NDVI-18.32*NDVI^2**	**7.745*exp(-22.8*NDVI)**	**-0.250+13.88*NDVI-20.43*NDVI^2**

Table 1. **Kernel coefficients used in CLARA-A1-SAL BRDF computation (Wu et al., 1995). NDVI = ($\rho_{\text{nir}} - \rho_{\text{red}}$)/($\rho_{\text{nir}} + \rho_{\text{red}}$).**

POSTPROCESSING METHOD FOR LARGE AEROSOL VALUES

The use of constant values for AOD at 550 nm (τ_{550}) enables postprocessing of the albedos to match thicker atmosphere, if the true values for τ_{550} are known. If the spectral albedo values of the red and visible channels were stored, it would be a straight forward exercise to remove the atmosphere used in CLARA-A1-SAL (τ_{550} = 0.1) and then replace it with the known atmosphere. However, at the time of the processing of the CLARA-A1-SAL time series it was not possible to store additionally the spectral albedo values globally for the whole time series. Therefore a simulation study is needed. For that purpose a data set was generated by varying the ρ_{TOA}, τ_{550}, θ_s, θ_v, $\Delta\varphi$, ozone and water vapour content values [*Table 2*]. The surface reflectance was calculated based on these values. Then the spectral albedo values and finally the broadband albedo value were determined using Eqs. 2 - 6. All combinations of the values of Table 1 were calculated, but unphysical results (i.e. $\rho_{red} < 0$, $\rho_{red} > 1$, $\rho_{nir} < 0$, $\rho_{nir} > 1$, $\alpha_{red} < 0$, $\alpha_{red} > 1$, $\alpha_{nir} < 0$, $\alpha_{nir} > 1$, $\alpha < 0$, $\alpha > 1$, $\rho_{red} > \rho_{nir}$) were excluded from the regression analysis. In addition, for the vegetated land cover classes it was required that NDVI exceeds 0.01, like in the SAL code. The calculations have not been carried out for atmospheres, for which $\tau_{550} > 1$, since the validity range of the SMAC atmospheric correction does not extend to extreme AOD values. The broadband albedo was also limited to be in the typical range, so that too high values were excluded. The limit values were 0.65 (barren), 0.4 (crop and forest) and 0.5 (grass). Thus the number of individual cases was reduced from 7 348 320 to 0.53 …1.4 million, depending on the land cover class. In addition, for barren land cover the calculations were carried out both for continental and desert atmosphere composition. Since the land cover class input used in the CM-SAF processing chain (USGS land cover map, Loveland et al., 2000) does not distinguish deserts, the SAL algorithm can't utilize the desert coefficients of the SMAC atmospheric correction. Therefore all areas are calculated using continental atmosphere. In Sahara, for example, this is obviously a source of additional error. Hence, it was also studied, how much changing the atmosphere from continental to desert affected the results of barren land cover.

Parameter	Values
ρ_{TOA}(red), barren	0.1, 0.2, 0.3, 0.4, 0.5, 0.6, 0.7, 0.8, 0.9
ρ_{TOA}(NIR), barren	0.1, 0.2, 0.3, 0.4, 0.5, 0.6, 0.7, 0.8, 0.9
ρ_{TOA}(red), crop	0.1, 0.2, 0.3, 0.4, 0.5, 0.6, 0.7, 0.8, 0.9
ρ_{TOA}(NIR), crop	0.1, 0.2, 0.3, 0.4, 0.5, 0.6, 0.7, 0.8, 0.9
ρ_{TOA}(red), forest	0.1, 0.2, 0.3, 0.4, 0.5, 0.6, 0.7, 0.8, 0.9
ρ_{TOA}(NIR), forest	0.1, 0.2, 0.3, 0.4, 0.5, 0.6, 0.7, 0.8, 0.9
ρ_{TOA}(red), grass	0.1, 0.2, 0.3, 0.4, 0.5, 0.6, 0.7, 0.8, 0.9
ρ_{TOA}(NIR), grass	0.1, 0.2, 0.3, 0.4, 0.5, 0.6, 0.7, 0.8, 0.9
θs (Degrees)	0, 10, 20, 30, 40, 50, 60, 70
θv (Degrees)	0, 10, 20, 30, 40, 50, 60
$\Delta\varphi$ (Degrees)	0, 10, 20, 30, 40, 50, 60,70 ,80 ,90, 100, 110, 120, 130, 140, 150, 160, 170
H_2O (cm)	0.25, 0.35, 0.5
O_3 (atm-cm)	0.5, 2.0, 3.5
τ_{550}	0.1, 0.2, 0.3, 0.4, 0.5, 0.6, 0.7, 0.8, 0.9, 1.0

Table 2*: *Values used for the input parameters of the simulations.

RESULTS

The correlation of the simulated broadband albedo at the true aerosol optical depth value at 550 nm wavelength τ_{550} and the albedo at the constant AOD value τ_{550} = 0.1 is shown for diverse land cover classes in Figure 1. The relatively complex BRDF of grass makes its albedo characteristics more complicated than that of the other land cover classes.

Simple regression equations were sought for the relationship between the albedo α_0 at τ_{550} = 0.1 (used in CLARA-A1-SAL calculations) and the albedo value α at various other values up to τ_{550} = 1 (*Table 3*). The regression variables were the albedo value at τ_{550} = 0.1 (α_0), the aerosol optical depth at 550 nm wavelength (τ_{550}), the sun zenith angle (θ_s), the satellite zenith angle (θ_v) and the azimuth angle difference of the sun and the satellite ($\Delta\varphi$). In many cases it turned out that α_0 and τ_{550} alone were sufficient information for retrieval of an accurate enough albedo estimate $\hat{\alpha}$ for thicker atmosphere. Because the SAL products are pentad or monthly mean values of 15 km x 15 km, the albedo values consist of contributions of several individual retrievals. Inevitably this means, that there is no unique triple of sun and satellite angular values related to the end product pixel. Correlation between α and α_0 was studied both taking into account the sun and satellite angle values and looking

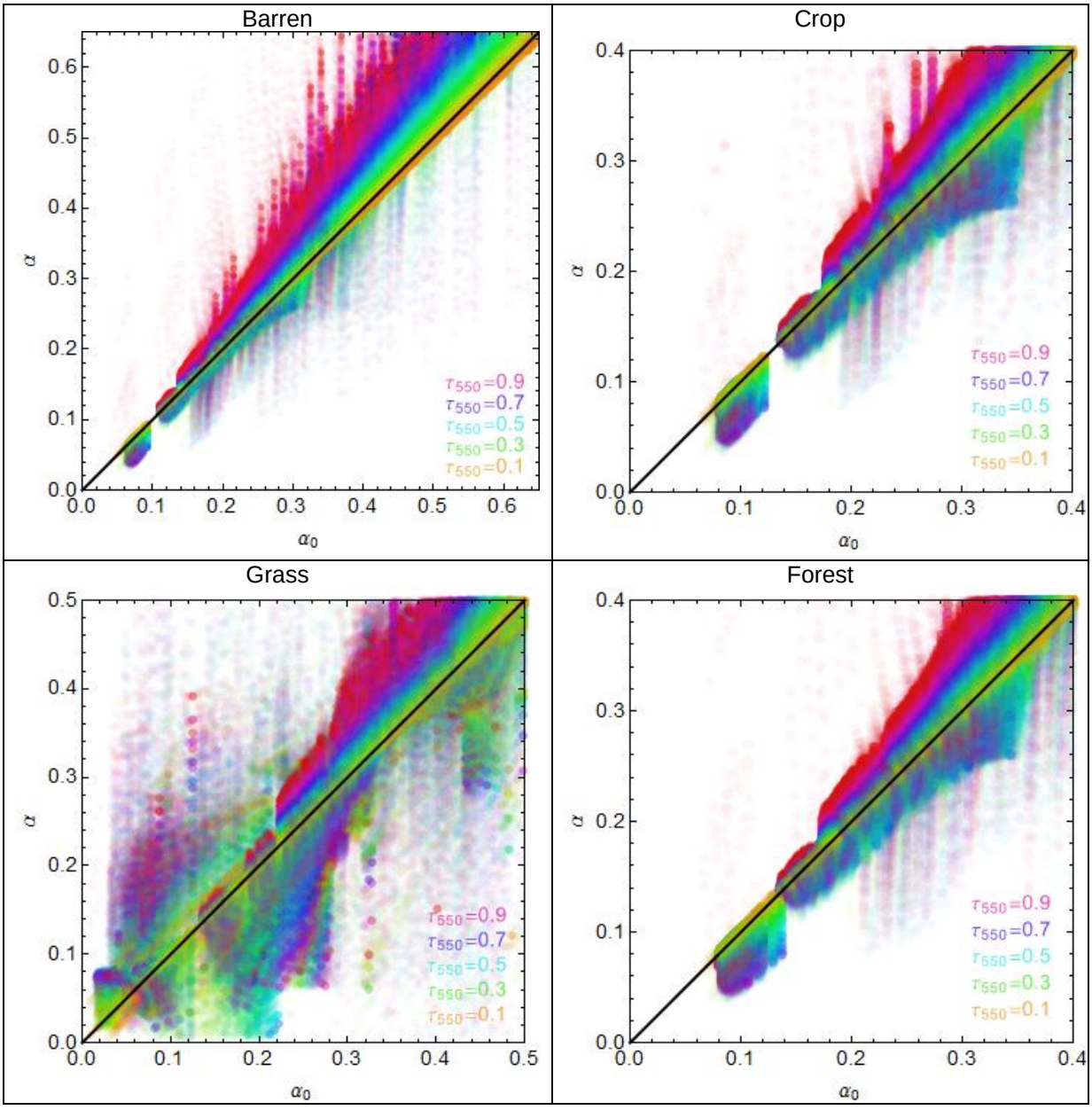

***Figure 1*. The relationship of the simulated broadband albedo α corresponding to varying τ_{550} value and the albedo α_0 corresponding to the constant aerosol optical depth value τ_{550} = 0.1 for land cover types barren, crop, forest and grass. In all cases the atmosphere parameters used in SMAC correction are continental. The intensity of the colours is related to the number of points. The same surface reflectance is the basis for the albedo values of all four land cover classes.**

Land cover type	Regression formula	$\lvert\hat{\alpha} - \alpha\rvert$ Median	$\lvert\hat{\alpha} - \alpha\rvert$ Q_{90}	$\lvert\hat{\alpha} - \alpha\rvert$ RMSE
Desert	$\hat{\alpha} = \alpha_0[1 + 0.0795645(\tau_{550} - 0.1)\exp(-\tau_{550} + 0.1)]$	**0.010**	**0.038**	**0.025**
Barren	$\hat{\alpha} = \alpha_0[1 + 0.36905(\tau_{550} - 0.1)\exp(-\tau_{550} + 0.1)]$	**0.007**	**0.035**	**0.024**
Cropland	$\hat{\alpha} = \alpha_0[1 + 0.137681(\tau_{550} - 0.1)\exp(-\tau_{550} + 0.1)]$	**0.007**	**0.032**	**0.019**
Forest	$\hat{\alpha} = \alpha_0[1 + 0.121082(\tau_{550} - 0.1)\exp(-\tau_{550} + 0.1)]$	**0.007**	**0.033**	**0.019**
Grassland	$\hat{\alpha} = \alpha_0[1 + 0.334268(\tau_{550} - 0.1)\exp(-\tau_{550} + 0.1)]$	**0.011**	**0.060**	**0.042**

Table 3. **Regression formulas for broadband albedo postprocessing of various land cover types. The corresponding root mean square error (RMSE) and median and 90% quantile (Q_{90}) values for the difference $\lvert\hat{\alpha} - \alpha\rvert$ are given as well.**

for a general relationship without explicit angular dependence. The sun and satellite zenith angles, however, affect the albedo values. Yet, it was mostly possible to find a reasonably accurate relationship between α and α_0 with only τ_{550} as an additional parameter. The reason for this is that the angles for the uncorrected and corrected albedo values of a pixel are exactly the same.

It would be desirable to have the broadband albedo estimation formulas in the form

$$\hat{\alpha} = \alpha_0[1 + \Delta((\tau_{550} - 0.1), \theta_s, \theta_v, \Delta\varphi...)] \quad (7)$$

so that the error term $\Delta((\tau_{550} - 0.1), \theta_s, \theta_v, \Delta\varphi)$ would be zero, when τ_{550} equals 0.1. It turned out, that it is really possible to achieve reasonable albedo estimation accuracy, when using only the aerosol optical depth information for postprocessing of the broadband albedo. For barren/desert, cropland and forest the accuracy was slightly better than for grassland (*Table 3*, *Figure 2*). This is probably due to the more complex BRDF of grassland. The RMSE values of the albedo estimation are shown as a function of the sun and satellite zenith angles in *Figure 2*. Obviously the postprocessing suffers from large sun and satellite zenith angles. This is natural, since the propagation of light becomes more complicated in those cases. The sun and satellite zenith angles affect the RMSE values slightly differently, because the SMAC algorithm is not completely symmetric to those angles. Including angular dependence in the postprocessing regression improved the albedo estimate accuracy only moderately. Largely this is because the angles are the same for the original albedo estimate and the postprocessed one. In addition, for large sun and satellite zenith angle values the atmospheric effect becomes very complex, as the path through the atmosphere is long, so that simple regressions will not catch the whole atmospheric characteristics.

For all land cover classes the postprocessed albedo accuracy decreases with increasing AOD. The postprocessing accuracy decreases markedly, when τ_{550} > 0.5. For very thick atmosphere the postprocessing is only partially able to remove the atmospheric contribution of the albedo value calculated using the constant value τ_{550} = 0.1 with desired accuracy. But one has to keep in mind, that in any case the albedo accuracy decreases with increasing AOD, because the atmospheric correction accuracy decreases, even when the precise AOD values are used in the albedo retrieval.

In addition to the simulated atmospheric data set (*Table 2*) a more realistic distribution of AOD, water vapour and total ozone amount values was derived from the monthly mean MODIS products (***Figure 3***).

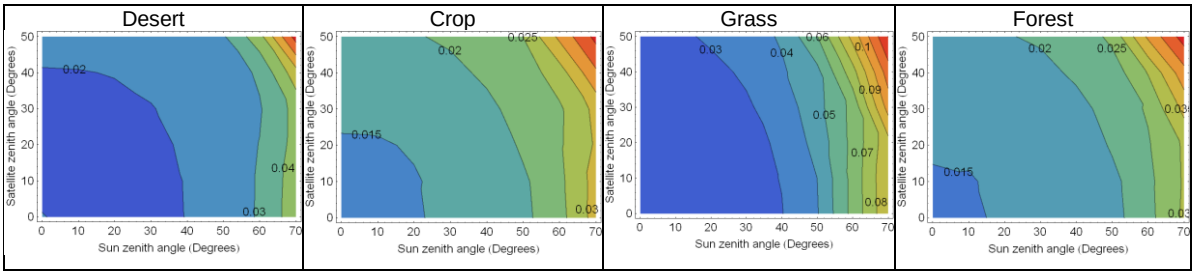

Figure 2. **The isocurves of the RMSE values of the $\lvert\hat{\alpha} - \alpha\rvert$ as a function of the sun and satellite zenith angles for the land cover classes desert, cropland, grassland and forest. The formulas of *Table 3* are used.**

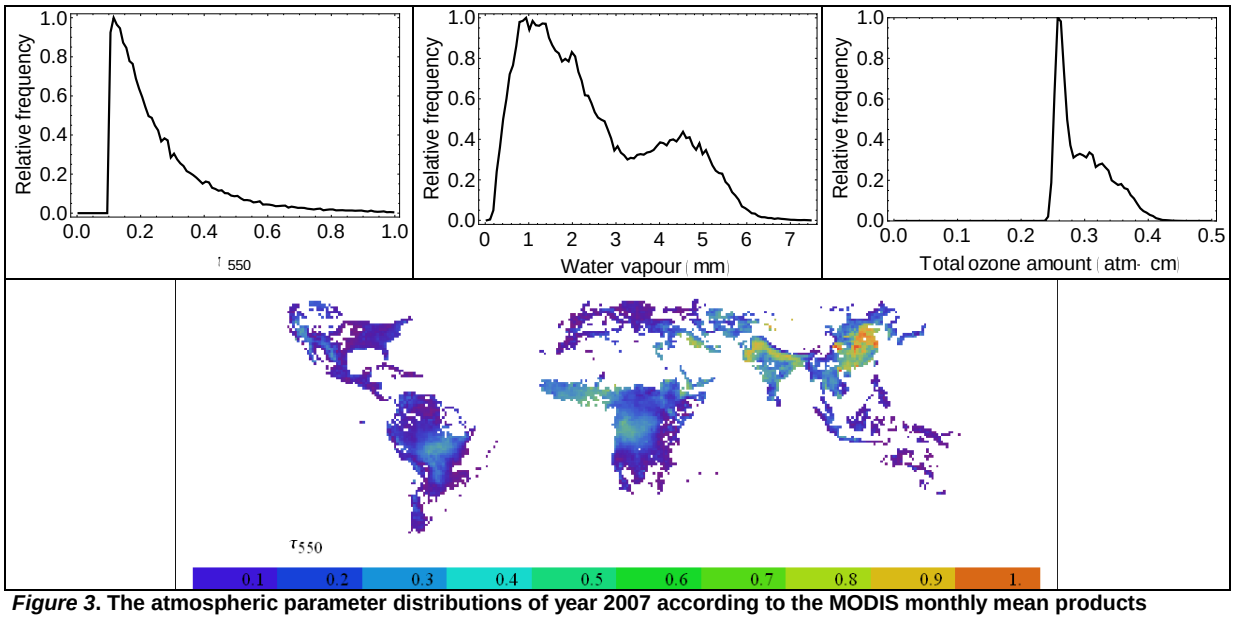

***Figure 3*. The atmospheric parameter distributions of year 2007 according to the MODIS monthly mean products (MOD08_M3). Only the pixels for which τ_{550} >0.1 are included.**

The global distribution of τ_{550} values exceeding 0.1 was first constructed. The distributions of the corresponding water vapour and total ozone mean values were derived too. The albedo calculations were carried out now anew by replacing the atmospheric parameters of *Table 2* with this new data set. The obtained regression parameters and accuracy statistics are given in *Table 4*.

The regression formulas of *Table 3* and *Table 4* were tested also by applying them to an observed case of thick atmosphere in India (***Figure 4***). The albedo was calculated for a NOAA/AVHRR image of January 1, 2007 (noaa17_20070101_0458) using the method as for the SAL product both for the constant atmosphere τ_{550} = 0.1 and for the mean AOD values of the daily mean MODIS products of January 1, 2007 (MOD08_D3.A2007001.005.2007004130642). The water vapour and ozone values were the mean values provided by the same MODIS product. The postprocessed albedo accuracy of the NOAA/AVHRR images turned out to be better when using the regression parameter values of *Table 3* (***Figure 5***). Only for forest the values of *Table 4* produced almost as good estimates (probably due to the large forest data set). It seems that using the monthly means of realistic atmosphere (***Figure 3***) as the basis of the regression (Eq. 7) did not contain enough variation to provide regression parameters suitable for independent real data, such as the two NOAA/AVHRR images. The big difference between the median and RMSE values of the postprocessed and true albedo value is caused by the error being dominated by the largest AOD values. Indeed, the postprocessing accuracy decreases with increasing AOD essentially linearly (*Table 5*).

As the CLARA-SAL product pixels typically contain contributions of several land cover classes, the postprocessing should be carried out as a linear combination of the land cover class dedicated regression formulas:

Land cover type	Regression formula	$\lvert\hat{\alpha}-\alpha\rvert$ Median	$\lvert\hat{\alpha}-\alpha\rvert$ Q_{90}	$\lvert\hat{\alpha}-\alpha\rvert$ RMSE
Desert	$\hat{\alpha}=\alpha_0\left(1-0.0436011(\tau_{550}-0.1)\exp(-\tau_{550}+0.1)\right)$	**0.005**	**0.016**	**0.012**
Barren	$\hat{\alpha}=\alpha_0\left(1-0.28381(\tau_{550}-0.1)\exp(-\tau_{550}+0.1)\right)$	**0.002**	**0.005**	**0.004**
Cropland	$\hat{\alpha}=\alpha_0\left(1+0.0781619(\tau_{550}-0.1)\exp(-\tau_{550}+0.1)\right)$	**0.002**	**0.012**	**0.009**
Forest	$\hat{\alpha}=\alpha_0\left(1+0.062814(\tau_{550}-0.1)\exp(-\tau_{550}+0.1)\right)$	**0.002**	**0.013**	**0.009**
Grassland	$\hat{\alpha}=\alpha_0\left(1+0.44027(\tau_{550}-0.1)\exp(-\tau_{550}+0.1)\right)$	**0.009**	**0.043**	**0.032**

***Table 4.* Regression formulas for broadband albedo postprocessing of various land cover types based on the MODIS AOD and water vapour data set. The corresponding root mean square error (RMSE) and median and 90% quantile (Q_{90}) values for the difference $|\hat{\alpha}-\alpha|$ are given as well.**

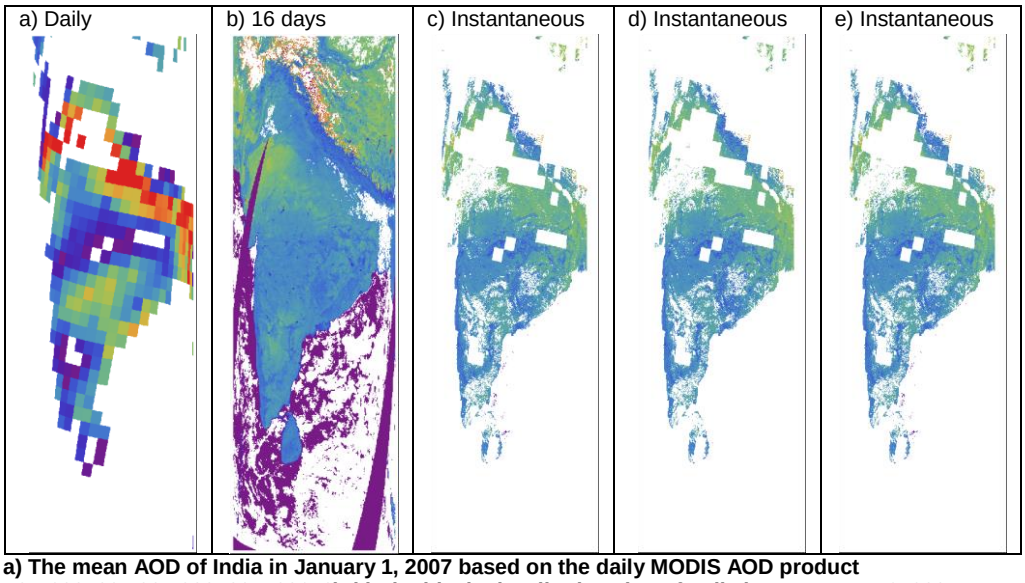

***Figure 4*. a) The mean AOD of India in January 1, 2007 based on the daily MODIS AOD product (MOD08_D3.A2007001.005.2007004130642). b) The black-sky albedo value of India in January 1-16, 2007 according to the MODIS product MCD43C3.A2007001.005.20070461064338. c) The calculated black-sky albedo of India in January 1, 2007 at 6:45 UTC based on the SAL algorithm and the AOD values of a). d) The calculated black-sky albedo of India in January 1, 2007 at 6:45 UTC based on the SAL algorithm and the constant AOD value τ_{550} = 0.1 and the correction formulas of *Table 3*. e) The calculated black-sky albedo of India in January 1, 2007 at 6:45 UTC based on the SAL algorithm and the constant AOD value τ_{550} = 0.1 and the correction formulas of *Table 4*.**

$$\hat{\alpha} \approx \alpha_0 \left[1 + \sum_{i=1}^{n} w_i c_i \left((\tau_{550} - 0.1) \exp(-\tau_{550} + 0.1) \right) \right] \qquad (8)$$

where the coefficients c_i are the land cover class specific regression parameter values of *Table 3* and the weights w_i are the fractions of the corresponding land cover classes. This equation is not precise, but as the individual land cover class fractions and related albedo values are not stored, and the land cover fractions taken into account in the original albedo estimate varies with cloud cover, this is considered a reasonable enough postprocessing estimation formula for the monthly mean and pentad SAL products. It is suggested to use the land cover fractions based on the USGS land cover map used in the SAL processing chain.

CONCLUSIONS

The accuracy of the CLARA-A1-SAL broadband albedo time series can be improved markedly in the areas of thick atmosphere by postprocessing, if the aerosol optical depth value is known. It is not necessary to use the sun and satellite zenith angle values in order to reach reasonable accuracy, but fractions of land cover classes should be taken into account. It is recommended to use a postprocessing method presented here (or corresponding approach) at areas typically having much higher AOD values than τ_{550} = 0.1.

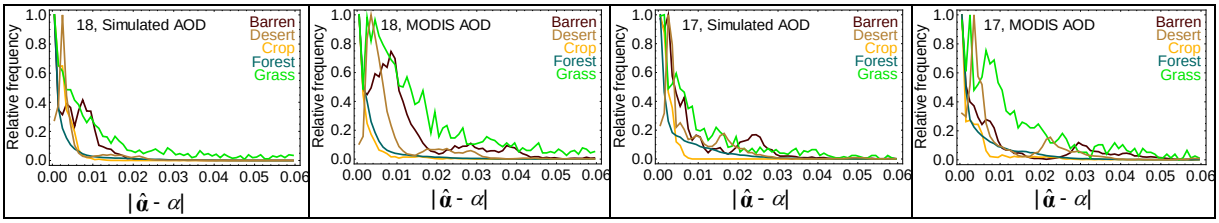

***Figure 5*. The distributions of $|\hat{\alpha} - \alpha|$ for the various land cover classes. Both the MODIS AOD product based and the simulated atmosphere were applied to the NOAA18/AVHRR image of January 1, 2007 at 6:45 UTC (*Figure 4*) and the NOAA17/AVHRR image of the same day taken at 04:58.**

Image	AOD	Land cover type	$\lvert\hat{\alpha} - \alpha\rvert$ Median	$\lvert\hat{\alpha} - \alpha\rvert$ Q_{90}	$\lvert\hat{\alpha} - \alpha\rvert$ RMSE	*n*	*c*	R^2
NOAA18	**Simulated**	**Barren**	**0.005**	**0.012**	**0.008**	**17178**	**0.018**	**0.82**
		Desert	**0.003**	**0.015**	**0.009**	**17178**	**0.016**	**0.47**
		Crop	**0.002**	**0.005**	**0.003**	**4106**	**0.010**	**0.94**
		Forest	0.002	0.013	0.009	108560	0.014	0.51
		Grass	**0.009**	**0.060**	**0.036**	**2234**	**0.051**	**0.55**
NOAA18	**MODIS**	**Barren**	0.008	0.030	0.018	15949	0.035	0.64
		Desert	0.005	0.022	0.013	15949	0.023	0.57
		Crop	0.001	0.007	0.006	3721	0.015	0.56
		Forest	**0.002**	**0.011**	**0.008**	**101733**	**0.012**	**0.52**
		Grass	0.012	0.068	0.039	2122	0.058	0.60
NOAA17	**Simulated**	**Barren**	**0.004**	**0.025**	**0.015**	**12241**	**0.029**	**0.63**
		Desert	**0.005**	**0.020**	**0.018**	**12241**	**0.033**	**0.59**
		Crop	**0.002**	**0.004**	**0.002**	**3377**	**0.009**	**0.94**
		Forest	**0.003**	**0.017**	**0.013**	**101791**	**0.022**	**0.49**
		Grass	**0.007**	**0.035**	**0.022**	**1081**	**0.046**	**0.64**
NOAA17	**MODIS**	**Barren**	0.006	0.039	0.026	11587	0.047	0.55
		Desert	0.005	0.028	0.021	11587	0.038	0.56
		Crop	0.002	0.014	0.008	3165	0.023	0.61
		Forest	0.003	0.028	0.014	96957	0.023	0.46
		Grass	0.010	0.040	0.024	1003	0.053	0.70

Table 5. **Statistics for the difference of the corrected albedo estimate and the true value calculated using the SAL algorithm and the AOD values based on MODIS (*Figure 3*). The number of observations *n* included in the statistics and the linear coefficient *c* and the coefficient of determination R^2 for the relationship $\lvert\hat{\alpha} - \alpha\rvert = c\,\tau_{550}$ *are* also given. The best alternatives are emphasized with bold red font.**

REFERENCES

Li, Z. Cihlar, J., Zheng, X., Moreau, L., and Ly, H, 1996, The bidirectional effects of AVHRR measurements over boreal regions. IEEE Transactions on Geoscience and Remote Sensing, **34**(6), 1308–1322.

Liang, S, 2000: Narrowband to broadband conversions of land surface albedo I: Algorithms. Remote Sensing of Environment, **76**, 213–238.

Loveland, T.R., Reed, B.C., Brown, J.F., Ohlen, D.O., Zhu, Z., Yang, L., and Merchant, J.W. Development of a global land cover characteristics database and IGBP DISCover from 1 km AVHRR data, International Journal of Remote Sensing, 21 (6-7), pp 1303-1330.

Rahman, H. and Dedieu, G., 1994, SMAC: a simplified method for the atmospheric correction of satellite measurements in the solar spectrum. International Journal of Remote Sensing, **15**, 123-143.

Riihelä, A., T. Manninen and K. Andersson, 2012, ”CM SAF Cloud, Albedo, Radiation dataset, AVHRR-based, Edition 1 (CLARA-A1), Surface Albedo, Algorithm Theoretical Basis Document”, SAF/CM/FMI/ATBD/GAC/SAL, 1.2, June 11, 2012, 57 p., DOI:10.5676/EUM_SAF_CM/CLARA_AVHRR/V001

Riihelä, A., Manninen, T., Laine, V., Andersson, K., and Kaspar, F., 2013, CLARA-SAL: a global 28 yr timeseries of Earth's black-sky surface albedo, Atmos. Chem. Phys., 13, 3743-3762, doi:10.5194/acp-13-3743-2013.

Roujean, J.L., Leroy, M., and Deschamps, P-Y., 1992, A bidirectional reflectance model of the earth’s surface for the correction of remote sensing data. Journal of Geophysical Research, **97**(18), 20455–20468.

Wu, A. Li, Z. and Cihlar, J., 1995, Effects of land cover type and greenness on advanced very high resolution radiometer bidirectional reflectances: Analysis and removal. Journal of Geophysical Research, **100**(D5), 9179–9192.